

### Evidence for Specific Solvation of Two Halocarbene Amides

Eric M. Tippmann,<sup>†</sup> Matthew S. Platz,<sup>\*,†</sup> Irina B. Svir,<sup>‡</sup> and Oleksiy V. Klymenko<sup>‡</sup>

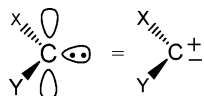
Contribution from the Department of Chemistry, The Ohio State University, 100 West 18th Avenue, Columbus, Ohio 43210, and Mathematical and Computer Modeling Laboratory, Kharkov National University of Radioelectronics, 14 Lenin Avenue, Kharkov, 61166, Ukraine

Received November 19, 2003; E-mail: platz.1@osu.edu

**Abstract:** Laser flash photolysis (LFP, 308 nm) of *endo*-10-halo-10'-*N,N*-dimethylcarboxamidetricyclo-[4.3.1.0]-deca-2,4-diene (**1C** and **1F**) releases indan and halocarbene amide (**2C** and **2F**). Although the carbenes are not UV-vis active, they react rapidly with pyridine to form ylides (**4C**, **4F**), which are readily detected in LFP experiments ( $\lambda_{\text{max}} = 450$  nm). Dioxane decreases the observed rate of carbene reaction with pyridine in  $\text{CF}_2\text{ClCFCl}_2$ . Small amounts of THF decrease the observed rate of reaction of carbene **2F** with pyridine but increase the rate of reaction of carbene **2C** with pyridine. LFP (266 nm) of dienes **1C** and **1F** in  $\text{CF}_2\text{ClCFCl}_2$  with IR detection produces carbenes **2C** and **2F** with carbonyl vibrations at 1635 and 1650  $\text{cm}^{-1}$ , respectively. In dioxane or THF solvent, LFP produces the corresponding ether ylides (**5C**, **5F**) by capture of carbenes **2C** and **2F**. The ylides have broad carbonyl vibrations between 1560 and 1610  $\text{cm}^{-1}$ . The addition of a small amount of dioxane in  $\text{CFCl}_2\text{CF}_2\text{Cl}$  extends the lifetime of the carbene. This observation, together with the ether-induced retardation of the rates of carbene capture by tetramethylethylene and pyridine, is evidence for solvation of the carbene by dioxane.

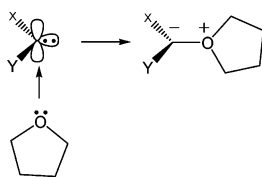
#### I. Introduction

Singlet carbenes have closed-shell singlet electronic configurations which have stimulated organic chemists to consider whether they might have zwitterionic character.<sup>1</sup>



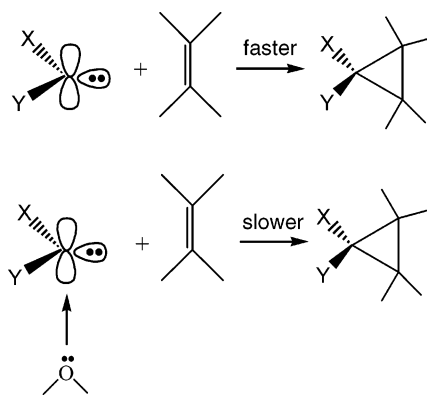
This in turn has led chemists to consider the possibility of specific solvation of carbenes, which involves weak (<5 kcal/mol) coordination of donating solvents such as ethers, nitriles, and aromatics to the empty p orbital of the carbene at distances greater than normal bond lengths.

One can immediately discern the difficulty in demonstrating specific solvation of carbenes because solvation of electrophilic carbenes with, for example, one or more molecules of an ether will lead to rapid collapse of the solvent complex (with a long C–O separation) to form a completely different species, an ylide, which in the case shown below, will have a normal carbon–oxygen bond length. The solvent complex may involve one or multiple ether ligands or, in the case of dioxane, bidentate ligands.



Less electrophilic carbenes may interact so weakly with coordinating solvents that specific solvation is either too weak to detect or nonexistent. This was our finding in two earlier studies of halophenylcarbenes.<sup>2</sup> Experimental and/or computational evidence for carbene solvent interactions has recently been presented by Khan and Goodman,<sup>3</sup> Ruck and Jones,<sup>4</sup> and Moss, Yan, and Krogh-Jespersen.<sup>5</sup> In earlier work, Tomioka and co-workers<sup>6</sup> reported dramatic effects of dioxane on the selectivity of arylcarbene reactions.

The simplest and most direct evidence of specific solvation would be the discovery of a unique spectroscopic signature of a specifically solvated carbene distinct from that of a free carbene and an ylide. We have not found such signatures in our reported work<sup>2</sup> or in this study. Thus, our approach will be indirect and focus on the influence of solvation on carbene dynamics. Our hypothesis will be that a specifically solvated carbene will undergo bimolecular reactions at a slower rate than a free carbene (Case 1).

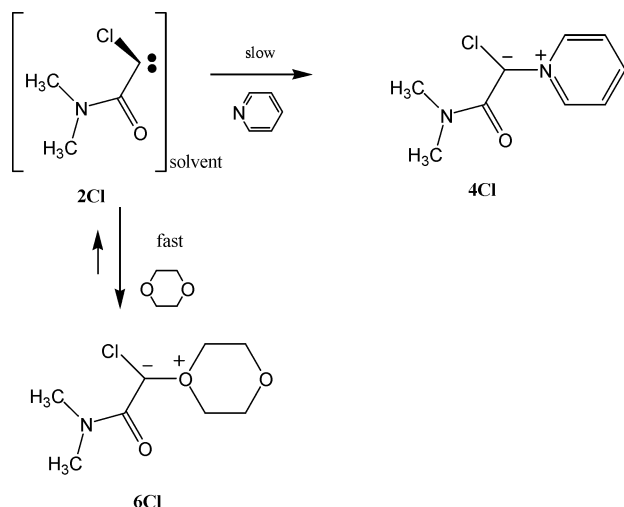


<sup>†</sup> The Ohio State University.

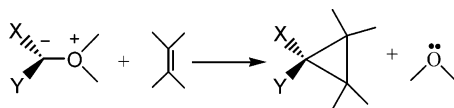
<sup>‡</sup> Kharkov National University of Radioelectronics.

(1) (a) Hoffmann, R. *J. Am. Chem. Soc.* **1968**, *90*, 1475. (b) Hoffmann, R.; Zeiss, G. D.; Van Dine, G. W. *J. Am. Chem. Soc.* **1968**, *90*, 1485.

The observation that a chelating solvent extends the lifetime of a carbene and reduces its reactivity will be consistent with specific solvation, but other explanations may also be possible. The same observation can be explained by rapid and reversible carbene-ether ylide formation. In this mechanism, the ylide acts as a reservoir that slowly releases free carbene that is subsequently trapped (Case 2).



A third explanation is also possible. The ylide itself might undergo bimolecular reactions reminiscent of carbene processes, but at a slower rate than the carbene reaction (Case 3). These ylide reactions might be mistaken for the faster carbene processes.

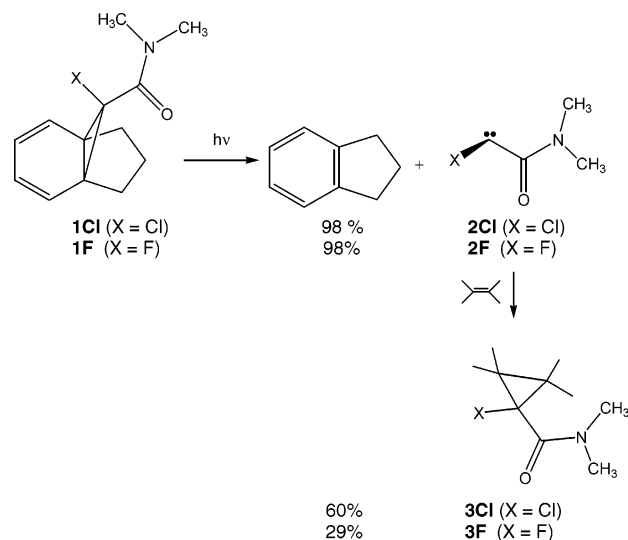


Thus, our results will be interpreted throughout in the context of cases 1–3.

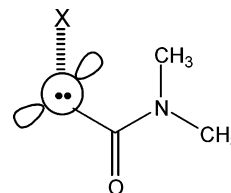
## II. Results

Dienes **1Cl** and **1F** were synthesized by simple extension of literature procedures.<sup>7,8</sup> The crystal structure of amide **1F** is presented in Supporting Information (Figure S1, Tables S1 and S2). Continuous photolysis (300 nm) of these dienes in neat tetramethylethylene (TME) produces indan and cyclopropanes **3Cl** and **3F**, consistent with the photochemical production of

halocarbene amides **2Cl** and **2F** in solution.



**II.1. Density Functional Theory (DFT) Calculations.** The minimum-energy geometries of carbenes **2Cl** and **2F** were calculated using the B3LYP level of theory with the 6-31G\* basis set.<sup>9</sup> The results resemble the data previously obtained with the related chlorocarbene ester<sup>8</sup> and are given in Figure S2 in Supporting Information. As expected, the plane defined by the carbonyl group and the amide nitrogen is nearly perpendicular to the plane defined by the halogen atom, carbene carbon, and the carbonyl carbon. This geometry allows the filled hybrid orbital of the carbene to conjugate with the  $\pi$  system of the carbonyl group. A methyl group of the amide moiety greatly shields one face of the carbene and blocks the approach of a nucleophile to one lobe of the empty p-orbital of the carbene.

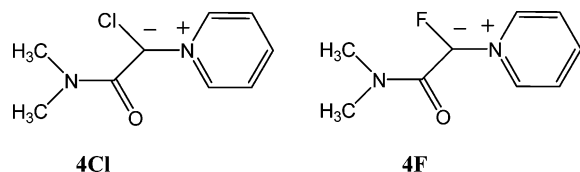


The predicted vibrational frequencies of the carbonyl group are at 1640  $\text{cm}^{-1}$  (**2Cl**) and at 1655  $\text{cm}^{-1}$  (**2F**) after scaling by a factor of 0.9613<sup>10</sup> (Figures S4 and S5, Supporting Information).

Time-Dependent Density Functional Theory (TD-DFT) calculations<sup>11</sup> predict vertical transitions of carbenes **2Cl** and **2F** that are summarized in Supporting Information, Tables S3 and S4. Neither carbene is predicted to absorb appreciably above 300 nm and should not be observed in laser flash photolysis (LFP) experiments with UV detection above 300 nm.

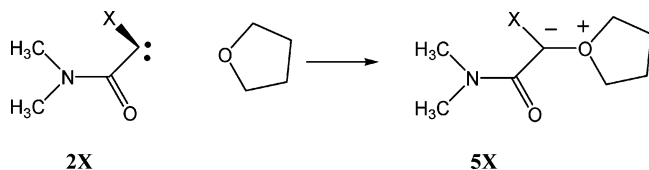
Many carbenes that lack useful UV–vis chromophores react with pyridine to form ylides that are readily detected.<sup>12</sup> The reactions of carbenes **2Cl** and **2F** with pyridine to form ylides **4Cl** and **4F** are predicted to be exothermic by 40 and 43 kcal/mol, respectively. In regards to the ylide geometries, the halogens are approximately 30° out of the plane formed by the amide group (Figures S6 and S7). This compares to a ground-state carbene in which the halogen is at 90° to the amide plane.

- (2) (a) Sun, Y.; Tippmann, E. M.; Platz, M. S. *Org. Lett.* **2003**, *5*, 1305. (b) Celebi, S.; Tsao, M.-L.; Platz, M. S. *J. Phys. Chem. A* **2001**, *105*, 1158.
- (3) Khan, M. I.; Goodman, J. L. *J. Am. Chem. Soc.* **1995**, *117*, 6635.
- (4) Ruck, R. T.; Jones, M., Jr. *Tetrahedron Lett.* **1998**, *39*, 2277.
- (5) Moss, R. A.; Yan, S.; Krogh-Jespersen, K. *J. Am. Chem. Soc.* **1998**, *120*, 1088.
- (6) Tomioka, H.; Ozaki, Y.; Izawa, Y. *Tetrahedron* **1985**, *41*, 4987.
- (7) (a) Banwell, M. G. *Aust. J. Chem.* **1988**, *41*, 1037. (b) Banwell, M. G.; Halton, B.; Hambley, T. W.; Ireland, N. K.; Papamihail, C.; Russell, S. G.; Snow, M. R. *J. Chem. Soc., Perkin Trans. 1* **1992**, *6*, 715.
- (8) (a) Likhovorik, I.; Zhu, Z.; Lee, E.; Tippmann, E.; Hill, B. T.; Platz, M. S. *J. Am. Chem. Soc.* **2001**, *123*, 6061. (b) Scott, A. P.; Platz, M. S.; Radom, L. *J. Am. Chem. Soc.* **2001**, *123*, 6069.
- (9) Ziegler, T. *Chem. Rev.* **1991**, *91*, 651.
- (10) Scott, A. P.; Radom, L. *J. Phys. Chem.* **1996**, *100*, 16502.
- (11) (a) Stratmann, R. E.; Scuseria, G. E.; Frisch, M. J. *J. Chem. Phys.* **1998**, *109*, 8218. (b) Casida, M. E.; Jamorski, C.; Casida, K. C.; Salahub, D. R. *J. Chem. Phys.* **1998**, *108*, 4439.
- (12) Jackson, J. E.; Platz, M. S. In *Advances in Carbene Chemistry*; Brinker, U., Ed.; JAI Press: Greenwich, CT, 1994; p 89.



TD-DFT calculations (B3LYP/6-311+G\*, Supporting Information Tables S5 and S6) predict that ylides **4Cl** and **4F** will absorb strongly at 383 and 376 nm, respectively, allowing them to be easily detected in LFP experiments with UV–vis detection.

DFT calculations (B3LYP/6-311+G\*) indicate that the reactions of **2Cl** and **2F** with THF to form ylides **5Cl** and **5F** are exothermic by 8 and 6 kcal/mol, respectively.



TD-DFT calculations of **5Cl** and **5F** predict that these ylides, unlike pyridine ylides **4Cl** and **5F**, will not absorb significantly above 300 nm (Tables S7 and S8, Supporting Information).

DFT calculations (B3LYP/6-31G\*) predict that the carbonyl vibrational frequencies of ylides **5X** will be very different from those of carbenes **2X**. The predicted frequencies are  $1563\text{ cm}^{-1}$  (**5Cl**) and  $1579\text{ cm}^{-1}$  (**5F**), after scaling by a factor of 0.9613.<sup>10</sup> The geometry of **5X** shows some significant changes relative to the carbene (Figures S8 and S9, Supporting Information). The halogen that was perpendicular to the amide plane in the carbene has a  $122^\circ$  dihedral angle (X–C–C–O) in the ylide. Also, the amide group is no longer planar. We will later conclude that the geometric changes that transpire in the amide group along the reaction coordinate between carbene and ylide are responsible for a small barrier to ylide formation.

**II.2. Laser Flash Photolysis Experiments with UV–Vis Detection.** Laser flash photolysis (LFP, 308 nm, 12 ns) of **1Cl** or **1F** in Freon-113 ( $\text{CF}_2\text{ClCFCl}_2$ ) fails to produce transient UV–vis spectra that can be attributable to carbenes **2Cl** or **2F** (Figures 1 and 2, respectively). As mentioned in the previous section, TD-DFT calculations indicate that this result is not surprising.

LFP of dienes **2Cl** and **2F** in the presence of pyridine produces intense new transient absorptions in the visible region (Figures 1 and 2). In Freon-113 and in cyclohexane, each transient is formed in an exponential process that can be analyzed to yield an observed rate constant  $k_{\text{OBS}}$ . The magnitude of  $k_{\text{OBS}}$  is linearly dependent on the concentration of pyridine (Figure 3). Thus, the carriers of the pyridine-dependent transient absorptions of Figures 1 and 2 are confidently associated with ylides **4Cl** and **4F**, consistent with previous experimental studies<sup>12</sup> and TD-DFT calculations.

As predicted, LFP of **1Cl** and **1F** in ethereal solvents such as THF and dioxane fails to produce UV–vis active transients (Figure S10). Carbenes **2Cl** and **2F** may well be reacting with ethers to form ylides **5X** and **6X** in these solvents, but if this is the case, these ylides must not absorb significantly above 300 nm.

Biphasic kinetics are uniquely observed upon LFP of **1Cl** in dioxane (Figure 4). Some pyridine ylide is formed rapidly, while

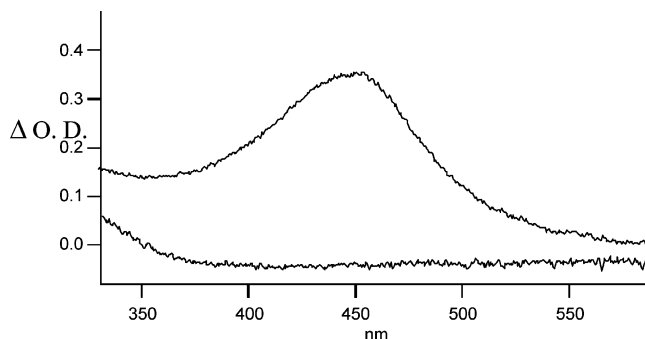


**Figure 1.** Transient spectrum produced by LFP (308 nm) of **1Cl** in Freon-113 (top, 1 M pyridine; bottom, 0 M pyridine). The spectrum was recorded 100 ns after the laser pulse over a window of 1  $\mu\text{s}$ .

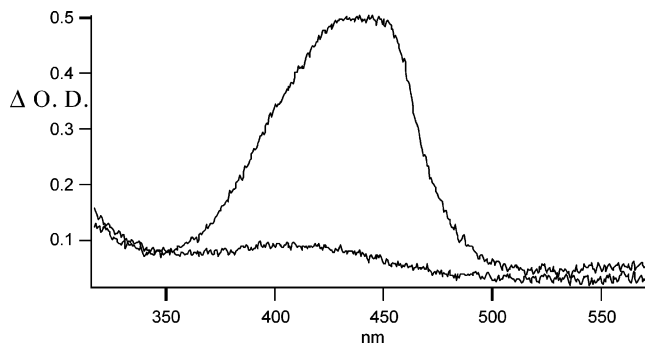


**Figure 2.** Transient spectrum produced by LFP (308 nm) of **1F** in Freon-113 (top, 1 M pyridine; bottom, 0 M pyridine). The spectrum was recorded 100 ns after the laser pulse over a window of 1  $\mu\text{s}$ .

a comparable amount is formed much more slowly at a concentration of pyridine of 0.62 M. The ratio of fast to slowly formed ylide varies with pyridine concentration. Increasing the pyridine concentration increases the yield of rapidly formed ylide. On the basis of TRIR studies (to be discussed later), we will conclude that the nascent carbene in neat dioxane partitions between reaction with pyridine to form **4Cl** and reaction with dioxane to form ylide **6Cl** in the fast step. The slow step, we believe, corresponds to the conversion of ether-ylide **6Cl** to pyridine ylide **4Cl** by a Case 2 or 3 mechanism.

The absolute rate constants of carbene reaction with pyridine ( $k_{\text{PYR}}$ ) as a function of solvent are collected in Tables 1 and 2 along with the carbene lifetimes ( $\tau \equiv 1/k_1$ , Scheme 1) deduced in these solvents in the absence of pyridine. In dioxane solvent, the effect of pyridine on the slow rate of ylide formation was analyzed. In the noncoordinating solvents cyclohexane and Freon-113 ( $\text{CF}_2\text{ClCFCl}_2$ ), the lifetimes of chlorocarbene **2Cl** are 1.1 and 1.6  $\mu\text{s}$  with  $k_{\text{PYR}}$  values of  $1.7 \times 10^8$  and  $1.5 \times 10^8\text{ M}^{-1}\text{ s}^{-1}$ , respectively (Figure 3). Values of  $k_{\text{PYR}}$  are only slightly reduced in benzene, dichloromethane, acetonitrile, and ethyl acetate, providing no impetus to invoke specific carbene–solvent interactions in these solvents. In dioxane (Figure S11, Supporting Information), however, the lifetime of the species (produced by LFP of precursor **1Cl**) that reacts with pyridine is extended to 18.9  $\mu\text{s}$  and  $k_{\text{PYR}} = 6.8 \times 10^5\text{ M}^{-1}\text{ s}^{-1}$ , a retardation of a factor of 221, relative to the  $k_{\text{PYR}}$  value in Freon-113! It was not possible to obtain  $k_{\text{PYR}}$  in THF or diethyl ether because pyridine ylide **4Cl** is formed faster than the time resolution of the spectrometer (10 ns) in these solvents at concentrations of pyridine that produce a reasonably intense signal. Carbene **2Cl** must react rapidly with THF and diethyl

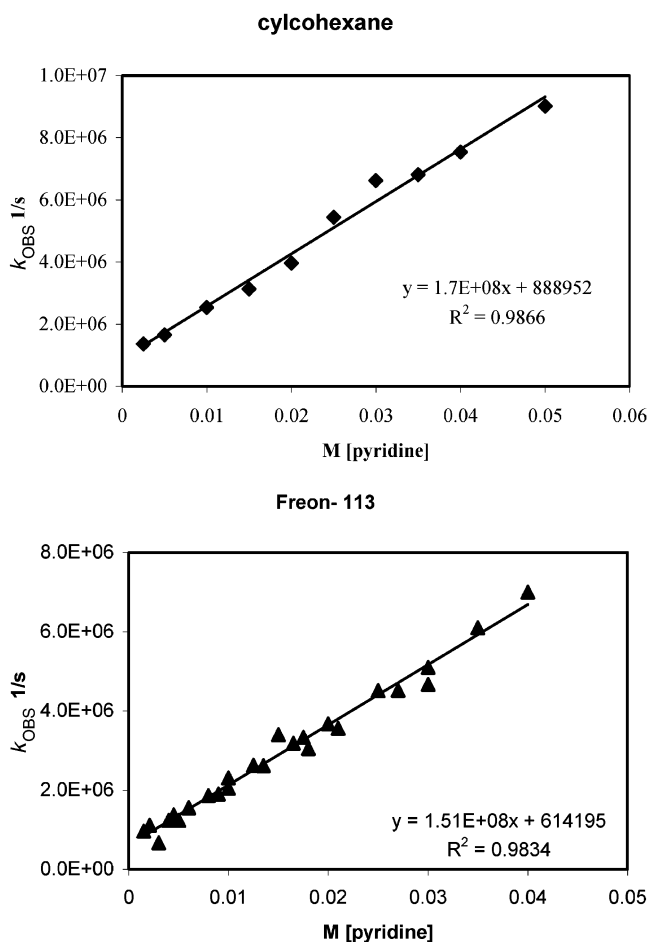


**Figure 3.** Plot of  $k_{\text{OBS}}$  of formation of ylide **4CI** versus pyridine concentration in cyclohexane and in Freon-113 at ambient temperature.

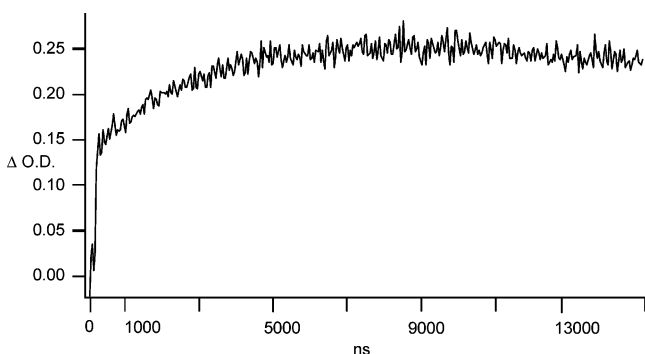


**Figure 4.** Biphasic formation of pyridine ylide **4CI** in dioxane produced by LFP of **1CI** in the presence of pyridine.

ether, and its lifetime in these two solvents must be rather short (<10 ns). If there is specific solvation of **2CI** in these two solvents, the complex must rapidly collapse.

Similar, but not identical, results were observed with the fluorocarbene amide **2F**. In Freon-113 and in cyclohexane, the carbene lifetimes are 0.9 and 0.5  $\mu\text{s}$  with  $k_{\text{PYR}}$  values of  $2.0 \times 10^9$  and  $2.8 \times 10^9 \text{ M}^{-1} \text{ s}^{-1}$ , respectively (Figure S12, Supporting Information). Once again,  $k_{\text{PYR}}$  is only slightly reduced in benzene and dichloromethane, and the carbene lifetime changes little relative to Freon-113. Large retardations of  $k_{\text{PYR}}$  are observed in diethyl ether, dioxane, and THF. Relative to Freon-113, reduction factors of  $k_{\text{PYR}}$  of 30, 24, and 244 are observed in these solvents, respectively. In contrast to **2CI**, the

lifetime of **2F** in the presence of pyridine is extended only slightly in dioxane. Again, in contrast with the chlorine analogue, the lifetime of **2F** in THF is not drastically shortened. In fact, the lifetime is slightly extended relative to Freon-113. It was not possible to obtain  $k_{\text{PYR}}$  with fluorocarbene amide **2F** in either ethyl acetate or acetonitrile because the carbene lifetime in these solvents is short (<10 ns). Specific solvation in these cases, if it exists, does not kinetically stabilize the carbene, and the rate of formation of ylide **4F** could not be resolved in these solvents.

Some observations presented in Tables 1 and 2 demand comment. Chelating solvents do not depress the absolute magnitude of the bimolecular rate constant of arylhalocarbenes with pyridine<sup>2</sup> or alkenes.<sup>13</sup> This is true as well with dichlorocarbene.<sup>14</sup> The observations that dioxane (with **2CI**) and THF (with **2F**) depresses  $k_{\text{PYR}}$  by 2 orders of magnitude is unprecedented. This result, taken in isolation, is equally consistent with Cases 1, 2, or 3.

It is remarkable that while THF and diethyl ether kinetically stabilize carbene **2F**, the same two ethers react extremely rapidly with carbene **2CI**. With one carbene, THF and diethyl ether form a kinetically stabilized complex or ylide, but with an analogous carbene, the same two ethers rapidly and irreversibly consume the pyridine-trappable reactive intermediate. Ethyl acetate and acetonitrile solvents kinetically stabilize **2CI**, but not **2F**. We cannot provide qualitative insight into this behavior. We can only conclude that we have not identified the subtle factor that leads one but not another carbene–solvent complex to rapidly collapse to form persistent products.

Finally, we note that fluorocarbene **2F** has larger absolute rate constants of reaction with pyridine than does **2CI** in all solvents examined. Arylchlorocarbenes are generally more reactive than arylfluorocarbenes.<sup>13,15</sup> This reactivity trend is not unprecedented, however. We have recently reported that carbomethoxyfluorocarbene<sup>16</sup> is more reactive than carbomethoxychlorocarbene.<sup>9a</sup> We pointed out that carbonyl substituents and aryl substituents interact with different orbitals of a singlet carbene, and we speculated that in the carbene esters, the electronegativity of fluorine overwhelms the  $\pi$  back-bonding property of fluorine, leading to an increase in electrophilicity.<sup>16</sup>

**Kinetics of Reaction of Carbenes **2CI** and **2F** with Tetramethylethylene.** Tetramethylethylene (TME) traps carbenes **2CI** and **2F** to form the expected cyclopropane products, **4CI** and **4F**, respectively. The presence of TME, at constant pyridine concentration, increases  $k_{\text{OBS}}$  and reduces the yield of the pyridine ylide. Plots of  $k_{\text{OBS}}$  versus [TME] are linear with slopes equal to  $k_{\text{TME}}$ , the absolute rate constant of carbene reaction with alkene (Figure 5). Values of  $k_{\text{TME}}$  are collected in Tables 3 and 4. It is clear that ethereal solvents dramatically reduce  $k_{\text{TME}}$  relative to Freon-113. The reactive intermediate produced by LFP of chloroamide precursor **1CI** reacts with tetramethylethylene 331 times more rapidly in Freon-113 than in dioxane. This observation is also unprecedented. Solvent has little reported influence on the absolute reactivity of arylhalocar-

(13) Moss, R. A.; Turro, N. J. In *Kinetics and Spectroscopy of Carbenes and Biradicals*; Platz, M. S., Ed.; Plenum: New York, NY, 1990; p 213.

(14) Presolski, S. I.; Zorba, A.; Thamattoor, D. M.; Tippmann, E. M.; Platz, M. S. *Tetrahedron Lett.* **2004**, *45*, 485.

(15) Gould, I. R.; Turro, N. J.; Butcher, J., Jr.; Doubleday, C., Jr.; Hacker, N. P.; Lehr, G. F.; Moss, R. A.; Cox, D. P.; Guo, W.; Munjal, R. C.; Perez, L. A.; Fedorynski, M. *Tetrahedron* **1985**, *41*, 1587.

(16) Tippmann, E. M.; Hologna, G.; Platz, M. S. *Org. Lett.* **2003**, *5*, 4919.

**Table 1.** Lifetime and  $k_{\text{PYR}}$  Values for **2Cl**

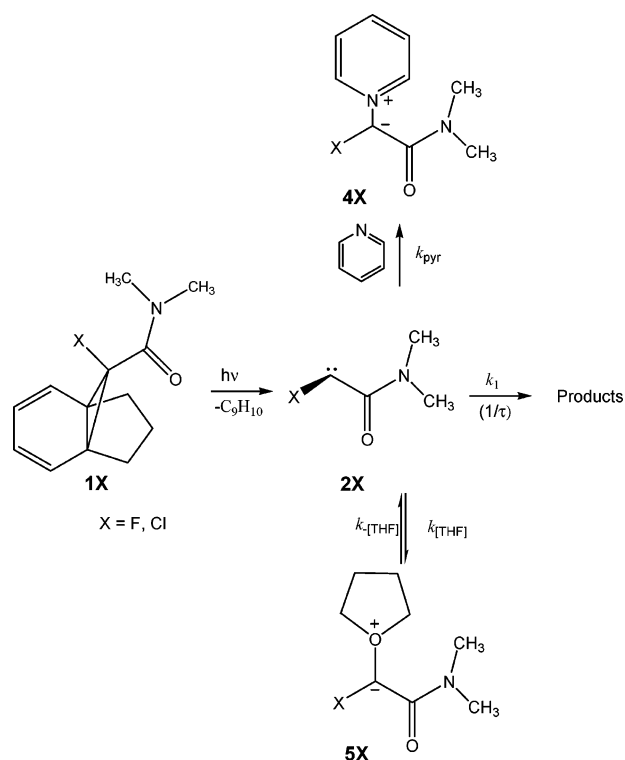
solvent	$\tau$ ( $\mu\text{s}$ )	$k_{\text{PYR}}$ ( $\text{M}^{-1} \text{s}^{-1}$ )	$k_{\text{PYR}}(\text{Freon-113})/k_{\text{PYR}}(\text{solvent})$
THF	a	a	a
dioxane	18.9	$6.8 \times 10^5$	221
ethyl acetate	0.8	$5.2 \times 10^7$	2.9
benzene	1.2	$7.2 \times 10^7$	2.1
$\text{CH}_2\text{Cl}_2$	1.7	$7.0 \times 10^7$	2.1
Freon-113	1.6	$1.5 \times 10^8$	1
cyclohexane	1.1	$1.7 \times 10^8$	0.9
acetonitrile	0.5	$6.7 \times 10^7$	2.2
diethyl ether	a	a	a

<sup>a</sup> Ylide formation cannot be resolved.

**Table 2.** Lifetime and  $k_{\text{PYR}}$  Values for **2F**

solvent	$\tau$ ( $\mu\text{s}$ )	$k_{\text{PYR}}$ ( $\text{M}^{-1} \text{s}^{-1}$ )	$k_{\text{PYR}}(\text{Freon-113})/k_{\text{PYR}}(\text{solvent})$
THF	2.6	$8.2 \times 10^6$	244
dioxane	1.3	$8.4 \times 10^7$	24
ethyl acetate	a	a	a
benzene	0.8	$8.3 \times 10^8$	2.4
$\text{CH}_2\text{Cl}_2$	1	$5.0 \times 10^8$	4
Freon-113	0.9	$2.0 \times 10^9$	1
cyclohexane	0.5	$2.8 \times 10^9$	0.7
acetonitrile	a	a	a
diethyl ether	0.9	$6.6 \times 10^7$	30

<sup>a</sup> Ylide formation cannot be resolved.

**Scheme 1**

benes<sup>2,13,15</sup> or dichlorocarbene<sup>14</sup> with alkenes. This result, taken again in isolation, is equally consistent with Cases 1, 2, or 3.

The temperature dependence of  $k_{\text{PYR}}$  for the reactive intermediates produced by LFP of fluoramide precursor **1F** was determined in two solvents. Arrhenius treatment of the data reveals that  $E_a$  is 0.72 kcal/mol and  $A$  is  $10^{6.8} \text{ M}^{-1} \text{ s}^{-1}$  in Freon-113 and that the value of  $E_a$  is 10.9 kcal/mol and  $A$  is  $10^{14.5} \text{ M}^{-1} \text{ s}^{-1}$  in THF (Figure S13, Supporting Information). It is obvious from the Arrhenius data that the mechanism changes between Freon-113 (free carbene) and THF. The larger activa-

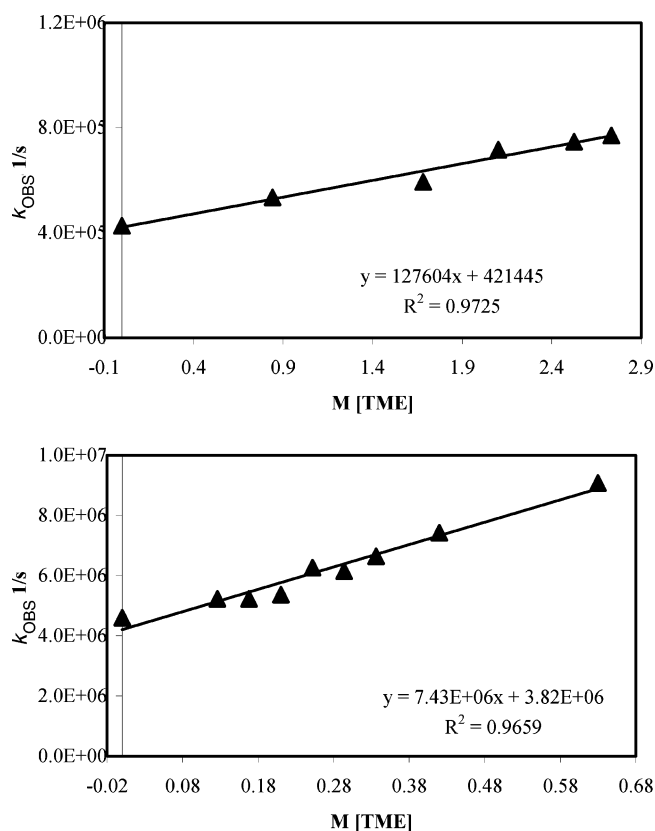


**Figure 5.** Plot of  $k_{\text{OBS}}$  of formation of ylides **4Cl** and **4F** versus tetramethylethylene concentration in dioxane at ambient temperature at constant (top: 0.62 M, bottom: 0.04 M) concentration of pyridine.

tion energy in THF relative to Freon-113 may simply reflect the kinetic advantage of a free carbene relative to solvated carbene (Case 1). It may simply be the free energy difference between ylide and carbene plus ether (Case 2). Or, it might reflect the difference in reactivity of a carbene (neat Freon-113) versus an ylide (neat THF) with pyridine (Case 3). At this point, the interpretations cannot be distinguished, but TRIR

**Table 3.** Values of  $k_{\text{TME}}$  of **2CI** at Ambient Temperature as a Function of Solvent<sup>a</sup>

solvent	$k_{\text{TME}}$ ( $\text{M}^{-1} \text{s}^{-1}$ )	$k_{\text{TME}(\text{Freon})}/k_{\text{TME}(\text{solvent})}$
Freon-113	$4.2 \times 10^7$	1
dioxane	$1.27 \times 10^5$	331

<sup>a</sup> Constant [pyridine] = 0.030 M (Freon-113); 0.62 M (dioxane).

**Table 4.** Values of  $k_{\text{TME}}$  of **2F** at Ambient Temperature as a Function of Solvent<sup>a</sup>

solvent	$k_{\text{TME}}$ ( $\text{M}^{-1} \text{s}^{-1}$ )	$k_{\text{TME}(\text{Freon})}/k_{\text{TME}(\text{solvent})}$
Freon-113	$1.99 \times 10^8$	1
$\text{CH}_2\text{Cl}_2$	$8.8 \times 10^7$	2.3
THF	$1.19 \times 10^7$	16.7
dioxane	$7.4 \times 10^6$	27

<sup>a</sup> Constant [pyridine] = 0.004 M (Freon-113); 0.0075 M ( $\text{CH}_2\text{Cl}_2$ ); 0.62 M (THF); 0.04 M (dioxane).

spectroscopic data will be used later to favor the latter two interpretations to explain the increased activation energy of pyridine ylide formation observed in neat THF.

**Influence of Small Amounts of Coordinating Solvents in Freon-113.** The influence of small amounts of acetonitrile and ethers on pyridine ylide formation was examined in Freon-113 and dichloromethane, which we presume to be noncoordinating solvents. Small amounts of acetonitrile both reduce the yield of pyridine ylide **4F** in dichloromethane and increase the rate of ylide formation ( $k_{\text{acetonitrile}} = 1.43 \times 10^7 \text{ M}^{-1} \text{ s}^{-1}$ ). This is the pattern one expects for reaction of **2F** with acetonitrile in competition with the reaction of the carbene with pyridine, assuming no effect of small amounts of acetonitrile on  $k_{\text{PYR}}$ . Small amounts of THF in Freon-113 again display the anticipated effect on the yield of pyridine ylide **4CI** and the rate of its formation (Figure S14). However, small amounts of THF decrease the rate of formation of pyridine ylide **4F** in Freon-113 (Figure 6).

The same unusual effect is observed with **2CI** and **2F** and dioxane (Figures 7 and 8). Small amounts of dioxane depress the rates of formation of ylides **4F** and **4CI** in Freon-113. Dioxane only slightly reduces the yield of pyridine ylide in this solvent. These results are not consistent with a mechanism in which the haloamide carbenes react with pyridine and dioxane to form ylides (or other products) at competitive rates. Such a mechanism requires that dioxane will increase the observed rate of formation of pyridine ylide, as observed with acetonitrile and TME.

These observations are again unprecedented. We know of no reagents that lengthen the lifetime of a carbene in solution and reduce its reactivity. We will use TRIR spectroscopy to demonstrate that this particular effect of dilute ether in Freon (unlike in neat ether solvent) cannot be explained by reversible carbene-ether ylide formation (Case 2) or by reaction of an ether ylide with pyridine (Case 3) and is indicative of specific solvation of carbene **2CI** (Case 1).

**II.3. Time-Resolved Infrared (TRIR) Spectroscopy.** LFP (266 nm) of dienes **1CI** and **1F** in Freon-113 produces the TRIR spectra shown in Figures 9 and 10. The spectra reveal the immediate bleaching of the precursor carbonyl vibration at  $1660 \text{ cm}^{-1}$  in both cases. New transients are formed within the time resolution (100 ns) of the spectrometer centered at 1635 and  $1650 \text{ cm}^{-1}$  upon LFP of **1CI** and **1F**, respectively. The lifetimes of the transients in various solvents are given in Table 5. As

the transient species decay, carbonyl bands attributable to the product of transient decay are not observed between 1600 and  $1660 \text{ cm}^{-1}$ . The stable reaction products formed upon photolysis of **1X** are likely to have carbonyl vibrations in the same region as the diene precursors and are therefore obscured.

DFT calculations (B3LYP/6-31G\*) predict that the carbonyl vibrations of chlorocarbene amide **2CI** and fluorocarbene amide **2F** will be observed (after scaling by a factor of 0.9613) at 1640 and  $1655 \text{ cm}^{-1}$ , respectively (Supporting Information Figures S2 and S3). Thus, the transients observed by TRIR in Freon-113 are assigned to carbene amides **2CI** and **2F**.

LFP of **1CI** in neat dioxane again reveals the bleaching of the precursor but, in addition, the formation of a broad absorption band between 1560 and  $1610 \text{ cm}^{-1}$  (Figure 11). This transient absorption is formed within 100 ns, the time resolution of the spectrometer. The broad absorption in dioxane at  $1580 \text{ cm}^{-1}$  decays with  $\tau = 18 \mu\text{s}$ . The “free” carbene ( $1640 \text{ cm}^{-1}$ ), observed in Freon-113 is not observed in neat dioxane 100 ns after the flash. The bleaching at  $1660 \text{ cm}^{-1}$  shows some recovery microseconds after the laser flash, evidence of the formation of a stable product with a carbonyl band similar to that of precursor **1CI**.

Very similar results were obtained upon LFP of **1CI** in THF and of **1F** in THF and dioxane. As mentioned previously, DFT calculations predict that carbenes **2CI** and **2F** will react exothermically with THF to form ylides **5CI** and **5F** ( $\Delta H = -8$  and  $-6 \text{ kcal/mol}$ , respectively). The calculations predict that the carbonyl vibrations of THF ylides **5CI** and **5F** will be observed at 1563 and  $1579 \text{ cm}^{-1}$ , respectively, after scaling by a factor of 0.9613.<sup>10</sup> Thus, we assign the bands observed by TRIR spectroscopy between 1550 and  $1600 \text{ cm}^{-1}$  in THF and dioxane to the corresponding ether-carbene ylides **5CI** and **5F**.

In dichloromethane solvent, “free” carbene **2CI** is observed at  $1620 \text{ cm}^{-1}$  and no broad absorption band is detected in the ylide region between 1580 and  $1600 \text{ cm}^{-1}$ . The presence of THF accelerates carbene decay in dichloromethane with  $k_{\text{THF}} = 1.6 \times 10^7 \text{ M}^{-1} \text{ s}^{-1}$  (Figure 12).

The presence of TME accelerates carbene decay in both dichloromethane and Freon-113. Plots of  $k_{\text{OBS}}$  versus [TME] are linear with slopes of  $k_{\text{TME}} = 1.2 \times 10^7 \text{ M}^{-1} \text{ s}^{-1}$  (Figure S15, Supporting Information) and  $1.9 \times 10^7 \text{ M}^{-1} \text{ s}^{-1}$  (Figure 15) for dichloromethane and Freon-113, respectively. These are consistent with the value of  $k_{\text{TME}}$  deduced using the pyridine ylide probe method in Freon-113 ( $4.2 \times 10^7 \text{ M}^{-1} \text{ s}^{-1}$ , Table 3), which further confirms our assignment of the TRIR spectrum observed in this solvent. It was not possible to determine  $k_{\text{TME}}$  in heptane because the carbonyl bands of the carbene and cyclopropane product overlap significantly in this solvent. Dioxane does not increase the rate of disappearance of **2CI** in heptane even at concentrations as large as 0.3 M (Figure S16, Supporting Information). We conservatively estimate that  $k_{\text{DIOXANE}}$  of **2CI**  $\ll 1 \times 10^6 \text{ M}^{-1} \text{ s}^{-1}$  in heptane from these observations. This observation rules out a Case 2 mechanism for noncoordinating solvents containing small amounts of dioxane. The reaction of the carbene with the ether is simply too slow for this mechanism to be operative.

In the previous section, we noted that small amounts of dioxane in Freon-113 decreased the rate of formation of pyridine ylide **4CI**. This could have been due to an influence of dioxane

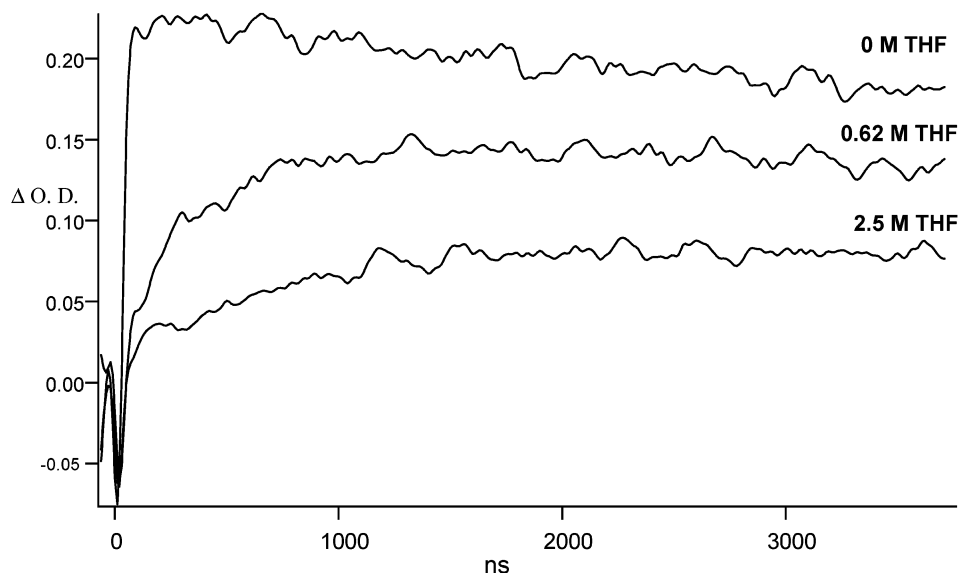


**Figure 6.** Effect of THF concentration on the yield of **4F** (constant 0.02 M pyridine) in Freon-113 and the rate of its formation at ambient temperature.

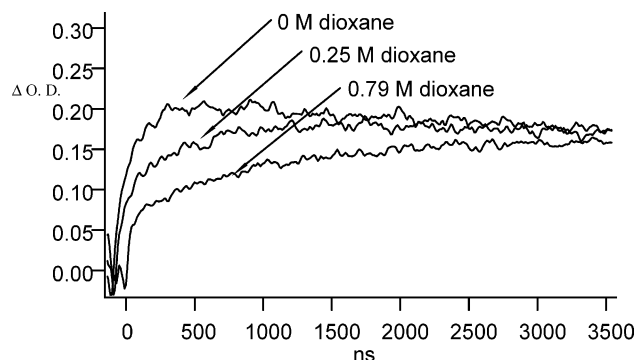


**Figure 7.** Effect of dioxane concentration on the yield of **4Cl** (constant 0.06 M pyridine) in Freon-113 and the rate of its formation at ambient temperature.

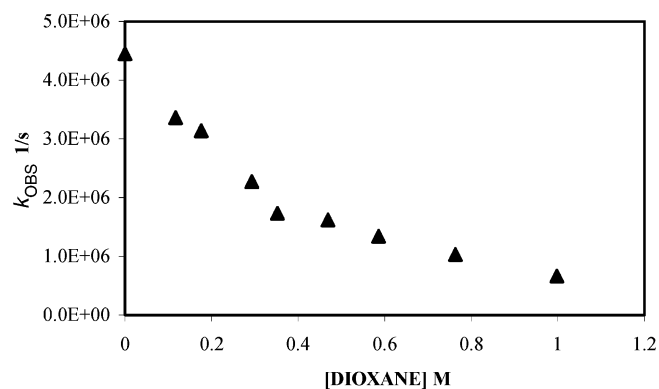


**Figure 8.** Effect of dioxane concentration on the value of  $k_{\text{OBS}}$  of **4Cl** (constant 0.06 M pyridine) in Freon-113 at ambient temperature.

on  $k_{\text{PYR}}$ , the absolute rate constant of carbene reaction with pyridine, or to an effect of ether on all non-pyridine-dependent pathways ( $k_1$ , Scheme 1). TRIR spectroscopy can probe this question, because unlike LFP with UV-vis detection, it allows direct observation of carbene **2Cl**.

The TRIR lifetime of carbene **2Cl** in Freon-113 is  $\sim 750$  ns. As shown in Figures 13 and 14, small amounts of dioxane extend the lifetime of the carbene. This demonstrates that the dioxane effect of Figure 7, observed by LFP in the presence of pyridine, is also observed in the absence of pyridine and that

dioxane must decrease the magnitude of  $k_1$  (Scheme 1). This result alone neither supports nor discredits the notion that small amounts of dioxane in Freon-113 reduce the absolute rate constant of carbene with pyridine,  $k_{\text{PYR}}$  (Scheme 1), for **2Cl**. Similar experiments are difficult to perform with fluorocarbene amide **2F** because its lifetime in Freon-113 is near the time resolution of the TRIR spectrometer.<sup>17</sup>

We attempted to determine the influence of small amounts of dioxane on  $k_{\text{TME}}$ , the absolute rate constant of reaction of carbene **2Cl** with tetramethylethylene. As mentioned previously, in Freon-113, in the absence of dioxane,  $k_{\text{TME}} = 1.9 \times 10^7 \text{ M}^{-1} \text{ s}^{-1}$ . The quality of the data becomes much poorer in the presence of dioxane, but as shown in Figure 15, small amounts of dioxane appear to reduce the magnitude of  $k_{\text{TME}}$  as expected for specific solvation (Case 1).

In Freon-113 containing 0.095 M THF, direct observation of both the lifetime of carbene **2Cl** ( $\sim 500$  ns) and the lifetime of THF ylide **5Cl** ( $\sim 5 \mu\text{s}$ ) is possible (Figure S17, Supporting Information). This result demonstrates that the carbene and the ylide are not in rapid equilibrium in Freon-113 containing dilute THF, relative to the reactions that consume these species, Case 2 is definitely not operative under these conditions. In Freon-113, the rate of formation of the broadly absorbing ylide at  $1580 \text{ cm}^{-1}$  (**5Cl**) can be resolved. The accuracy in the growth rate constant is poor, but it is on the order of 100 ns. The data are consistent with decay of carbene ( $1630 \text{ cm}^{-1}$ ) to form the  $1580 \text{ cm}^{-1}$  absorbing transient. Thus, the kinetic data is consistent with the computational results and indicates that the carrier of the  $1580 \text{ cm}^{-1}$  transient absorption is THF ylide **5Cl** in Freon-113.

In Freon-113 containing 0.062 M dioxane, photolysis of **1Cl** produces a broadly absorbing transient from  $1640$  to  $1576 \text{ cm}^{-1}$  with a maximum at  $1635 \text{ cm}^{-1}$  (Figure S18, Supporting Information). Unlike the related experiment with THF, there are not two kinetically distinct species attributable to carbene

(17) Lifetimes of **2Cl** and **2F** in Freon-113 are controlled by bimolecular processes, including the reaction of carbene with precursor. The concentrations of precursors **1X** used in the TRIR experiments are 10–20 times larger than in LFP experiments (because of the small path lengths in TRIR); thus, the lifetimes of the carbenes differ significantly between the two time-resolved experiments.

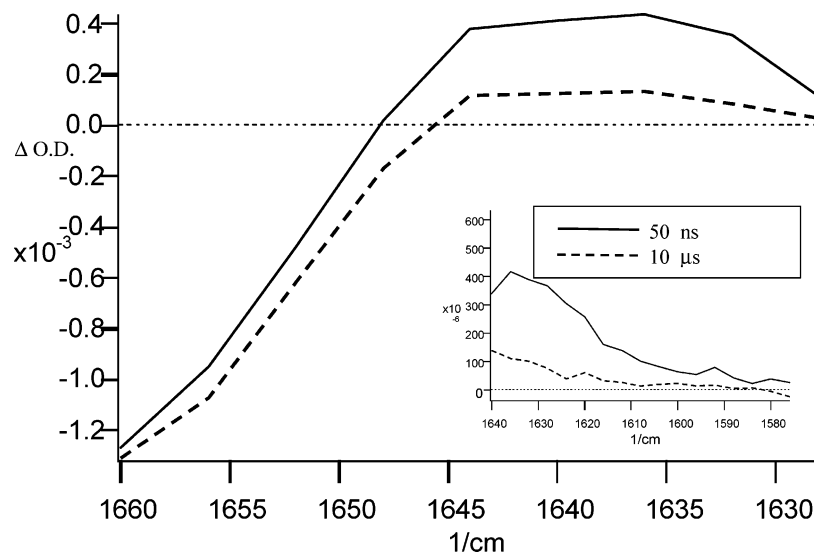


**Figure 9.** Transient IR spectrum produced upon LFP (266 nm) of **1CI** in Freon-113 at ambient temperature.



**Figure 10.** Transient IR spectrum produced upon LFP (266 nm) photolysis of **1F** in dioxane at ambient temperature.

**Table 5.** TRIR Determined Lifetime Values for **2CI** and **2F** in Various Solvents

solvent	<b>2CI</b> , lifetime ( $\tau$ )	<b>2F</b> , lifetime ( $\tau$ )
Freon-113	750–833 ns	200 ns
CH <sub>2</sub> Cl <sub>2</sub>	590–710 ns	N/A
Benzene	650 ns	N/A

and ylide. The kinetic profile from 1640 to 1576 cm<sup>-1</sup> is homogeneous across the entire region, and no new transient is observed for carbene-dioxane ylide **6CI**. Increasing the concentration of dioxane gradually shifts the spectrum to that of Figure 11 where only the ylide is observed at 1580 cm<sup>-1</sup>. In Freon-113 containing 0.062 M dioxane, the weak absorption of carbene between 1580 and 1600 cm<sup>-1</sup> must exceed that of the ylide, which must be present in only trace quantities. Finally, if we closely examine both the TRIR results and those obtained by LFP using the pyridine ylide method, we find that their results mirror one another quite well.

**Bimolecular Reactions of Ether Ylides?** The broadly absorbing ylide at 1580 cm<sup>-1</sup> obtained by LFP of diene **1CI** in ether solvent reacts with piperidine ( $k_{\text{PIP}} = 2.3 \times 10^7 \text{ M}^{-1} \text{ s}^{-1}$ , THF;  $k_{\text{PIP}} = 7.4 \times 10^6 \text{ M}^{-1} \text{ s}^{-1}$ , dioxane) and less rapidly with TME ( $k_{\text{TME}} = 1.8 \times 10^6 \text{ M}^{-1} \text{ s}^{-1}$ , THF;  $k_{\text{TME}} = 4.8 \times 10^5 \text{ M}^{-1} \text{ s}^{-1}$ , dioxane). The broadly absorbing transient produced by LFP

of diene **1F** in THF reacts similarly ( $k_{\text{TME}} = 2.8 \times 10^7 \text{ M}^{-1} \text{ s}^{-1}$ , THF). It was not possible to measure  $k_{\text{PYR}}$  for the reaction of the broadly absorbing transients in ethereal solvent with pyridine by TRIR spectroscopy, due to the strong absorption of pyridine at 266 nm, the wavelength of the exciting laser pulse.

In principle, piperidine may react with ylide **5CI** in one of three ways (pathways a–c, Scheme 2) in a Case 3 mechanism. If piperidine attacks the ylidic carbon atom, it must approach from out of the plane, as the backside of the ylide is shielded by the dimethylamide group. Piperidine may also serve as a base in an E<sub>2</sub> process (pathway c, Scheme 2). Piperidine will also accelerate the decay of ylide **5CI** if the ylide is in rapid equilibrium with the free carbene (Scheme 1) in neat dioxane.

### III. Discussion

**III.1. Influence of Dioxane.** The TRIR data demonstrate that dioxane extends the lifetime of carbene **2CI**. Solvation of the carbene must stabilize the intermediate and reduce its reactivity in Freon-113 as expected in a Case 1 mechanism. This result explains the influence of small amounts of dioxane on the observed rate constant of pyridine ylide formation. It is possible, however, that dioxane influences both  $\tau$  and  $k_{\text{PYR}}$  in these experiments. To probe this point, we deconvoluted the observed rate constants of reaction of carbene **2CI** with pyridine (to form ylide **4CI**) into best fit values of  $k_1$  ( $1/\tau$ , Scheme 1) and  $k_{\text{PYR}}$  ( $k_2$ , Scheme 1) using the program KinFitSim.<sup>18–20</sup> This software package is designed to simulate homogeneous chemical processes and the fitting of experimental data to a user defined mechanism. It automatically derives the mathematical model of the reaction scheme (a system of ordinary differential equations) and solves it using either the Gear or Runge–Kutta methods, which yields the concentration distributions of all species taking part in the kinetic system. To fit the experimental data, the user can convert the concentrations of the species into the experimentally measured quantity (for example, absorbance) by defining the corresponding equation and choosing the

(18) Svir, I. B.; Klymenko, A. V.; Platz, M. S. *Radioelectronika i Inform.* **2001**, *1*, 132.

(19) Svir, I. B.; Klymenko, A. V.; Platz, M. S. Management Information: Systems and Devices. *All-Ukr. Sci. Interdep. Mag.* **2001**, *116*, 24.

(20) Svir, I. B.; Klymenko, O. V.; Platz, M. S. *Comput. Chem.* **2002**, *26*, 379.



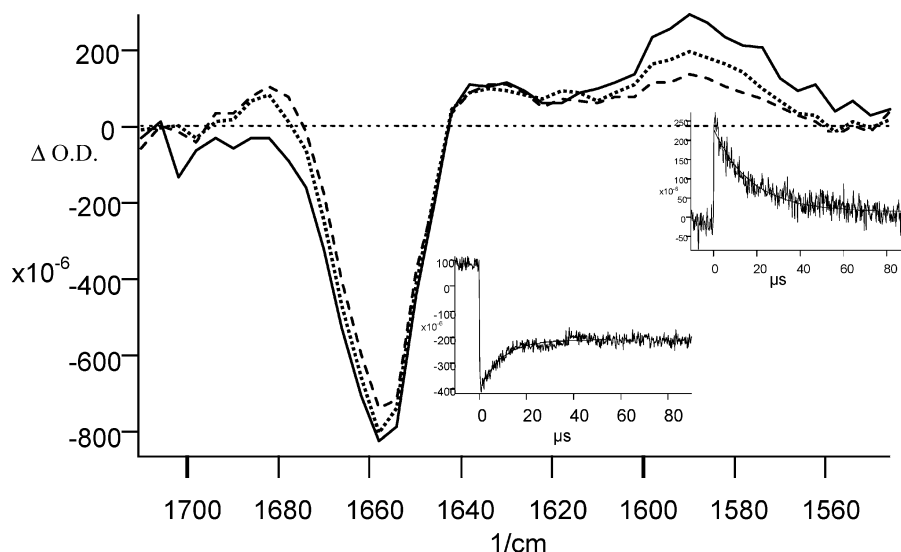


**Figure 11.** Transient IR spectrum produced upon LFP (266 nm) photolysis of **1CI** in dioxane at ambient temperature.

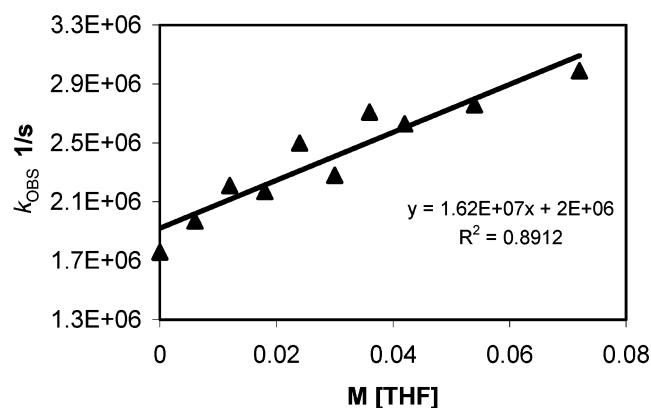


**Figure 12.** Plot of  $k_{\text{OBS}}$  versus  $M$  [THF] for **2CI** ( $1635\text{ cm}^{-1}$ ) in dichloromethane at ambient temperature.

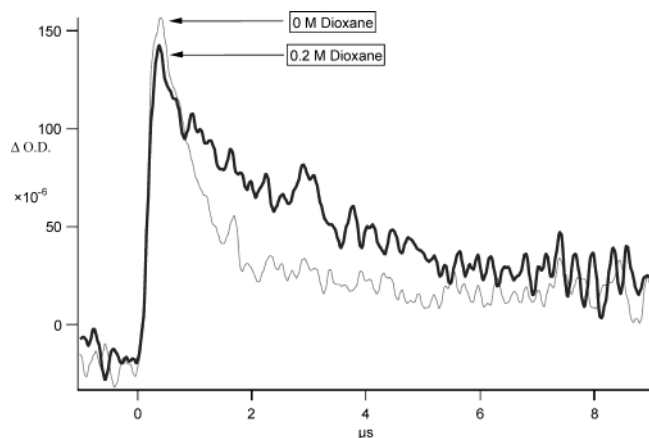


**Figure 13.** Influence of dioxane on the observed rate of decay ( $k_{\text{OBS}}$ ) at **2CI** ( $1635\text{ cm}^{-1}$ ) as a function of [dioxane].

parameters to be optimized. Then, the experimental data can be loaded, and an automatic fitting procedure can be used to obtain the best-fit parameters of the experimental data. The fitting simulator uses the steepest descent, Gauss–Newton, or Marquardt methods to find the best fit between the simulated and experimental curves.

Deconvolution was performed using the experimentally determined growth of pyridine ylide **4CI** in Freon-113 as a

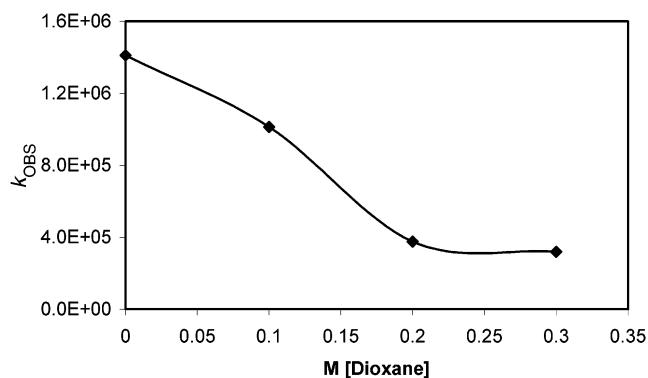


**Figure 14.** Influence of dioxane on the observed rate constant of disappearance of carbene **2CI**, monitored by TRIR at  $1635\text{ cm}^{-1}$  in Freon-113.

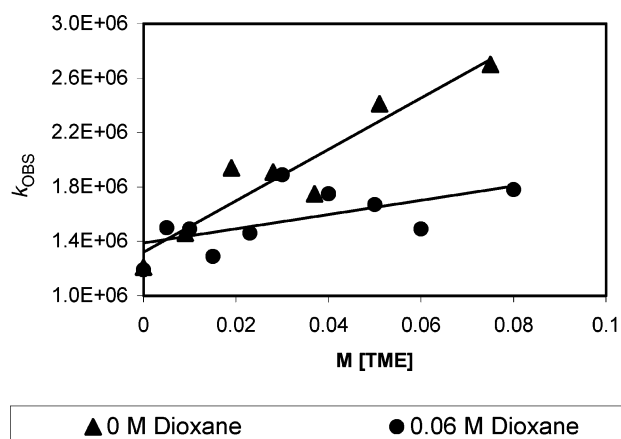
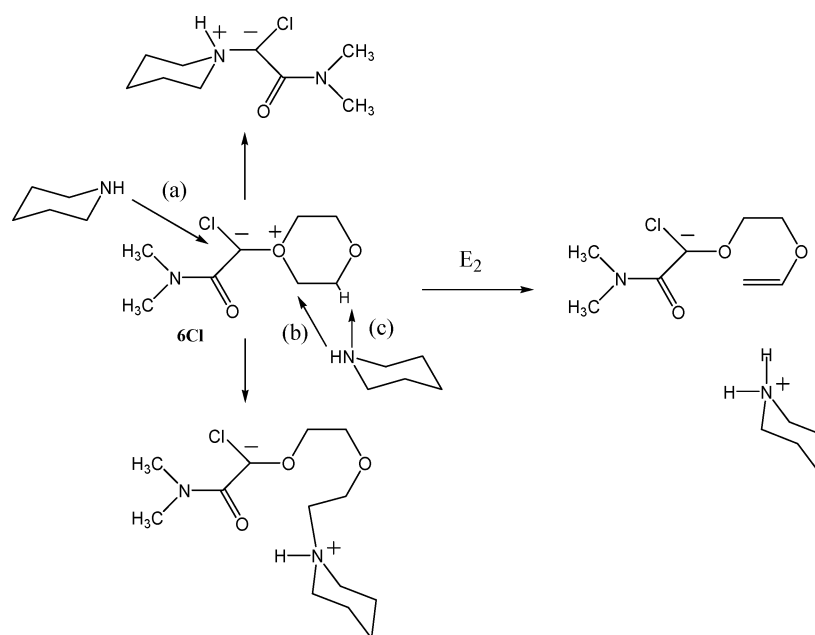


**Figure 15.** Plot of  $k_{\text{OBS}}$  versus the concentration of TME in Freon-113 for **1CI**.

function of dioxane concentration. In this analysis, we made two assumptions: (1) that only ylide **4CI** absorbs at 450 nm and (2) that the dioxane-solvated carbene **2CI** forms ether ylide **6CI** much more slowly than it reacts with 0.06 M pyridine to form ylide **4CI**. The latter assumption is valid because TRIR spectroscopy reveals that  $k_{\text{DIOXANE}}(\mathbf{2CI})$  is less than  $10^6\text{ M}^{-1}\text{ s}^{-1}$  (Figure 14, Freon-113, and Figure S16, heptane, Supporting Information).

Scheme 2



The kinetic mechanism shown in Scheme 1 was then abbreviated in the KinFitSim format as the following:



where  $A$  is solvated carbene  $2Cl$ ,  $B$  represents the sum of all pseudo-first-order and first-order products of carbene decay in Freon-113 in the absence of pyridine and ether,  $C$  is pyridine,  $D$  is pyridine ylide  $4Cl$ ,  $E$  is dioxane, and  $F$  is carbene-dioxane ylide  $6Cl$  (Scheme 1). The rate constants are  $k_1 = 1/\tau$  the sum of all first-order and pseudo-first-order rate constants of carbene decay in Freon-113 in the absence of pyridine and ether;  $k_2 = k_{PYR}$ ;  $k_{+3} = k_{DIOXANE}$ ; and  $k_{-3} = k_{-DIOXANE}$  the rate constants of conversion of solvated complex to ylide, and reversion of the ylide to solvated carbene. The Gear method was used for the simulation of the kinetic scheme, and the steepest descent method was used for fitting the experimental data. We analyzed the absorbance data obtained for concentrations of carbene  $2Cl$  of  $\sim 10^{-4}$  M and of pyridine of 0.06 M with varying concentrations of ( $E$ ).

We also analyzed the pyridine ylide forming data of  $2F$  with THF and dioxane. The results are very similar to those obtained with  $2Cl$  and dioxane and for that reason will not be presented.

As shown in Figure 16, increasing the concentration of dioxane in Freon-113 smoothly decreases  $k_1$  ( $\equiv 1/\tau$ ) where  $\tau$  is the carbene-solvent complex lifetime. The best-fit results of the LFP experiments are in qualitative agreement with the TRIR data. Quantitative agreement is not expected because the LFP and TRIR experiments use different precursor concentrations. As carbene reacts with precursor, the carbene has a shorter lifetime in the more concentrated solutions used in TRIR spectroscopy.<sup>17</sup> Figure 17 reveals that 0.1 M dioxane has little influence on  $k_{PYR}$  but that  $k_{PYR}$  ( $\equiv k_2$ ) decreases sharply at

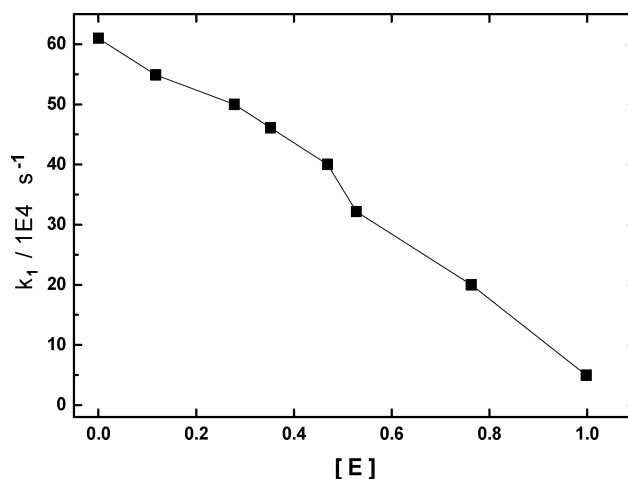
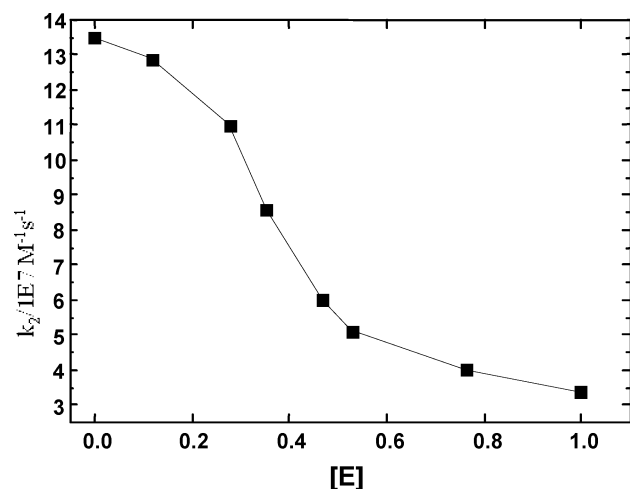


Figure 16. Computed variation in  $k_1(1/\tau)$  in Freon-113 as a function of [dioxane].

dioxane concentrations between 0.2 and 0.5 M. As the concentration of dioxane increases beyond 0.5 M, there is little additional decrease in  $k_{PYR}$ . These results are reminiscent of the influence of small amounts of hydrogen bonding agents on the kinetics of  $SN_2$  reactions in dipolar aprotic solvents.<sup>21</sup>

This analysis indicates that small amounts ( $<0.2$  M) of dioxane do not lead to a carbene solvent complex that has different values of  $\tau$  and  $k_{PYR}$ . At dioxane concentrations between 0.2 and 0.5 M, a carbene-solvent complex is formed that reacts with pyridine more slowly than the free carbene. Adding additional dioxane beyond 0.5 M has little influence on the reactivity of the carbene-solvent complex and presumably its structure. These results suggest to us that more than a single dioxane molecule may be needed to interact with carbene  $2Cl$  in such a way as to significantly alter the solvent carbene lifetime and the rate constant of its reaction with pyridine relative to free carbene.

(21) Heyding, R. D.; Winkler, C. A. *Can. J. Chem.* **1951**, *29*, 790.



**Figure 17.** Computed variation in  $k_2(k_{\text{PYR}})$  in Freon-113 as a function of [dioxane].

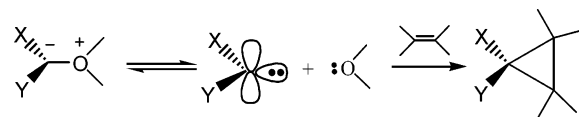
**III.2. Reversible Ylide Formation?** It is possible to deconvolute the experimental data used in the previous section with KinFitSim, according to a Case 2 mechanism that involves the reversible formation of an ether ylide as shown in Scheme 1. We will first assume that on the time scales of these experiments that only free carbene reacts with pyridine and undergoes decomposition and that the ether ylide **6Cl** neither reacts with pyridine nor decomposes during the lifetime of the carbene. Values of  $k_{\text{DIOXANE}}$  of  $4\text{--}5 \times 10^9 \text{ M}^{-1} \text{ s}^{-1}$  (**2Cl**) and  $k_{\text{DIOXANE}}$  of  $2\text{--}3 \times 10^9 \text{ s}^{-1}$  (**2F**) are obtained when we assume that  $1/\tau = 6.3 \times 10^5 \text{ s}^{-1}$  and  $k_{\text{PYR}} = 1.5 \times 10^8 \text{ M}^{-1} \text{ s}^{-1}$  (values determined in Freon-113 in the absence of dioxane) and are not allowed to vary.

This analysis (Case 2) requires a fast equilibrium between ether solvated carbene and ether ylide, relative to the rate of reaction of carbene with ylide. In this scenario, the ether ylide serves as a reservoir for the carbene, which subsequently reacts with pyridine. Dioxane slows the rate of formation of pyridine ylide by immediately diverting nascent carbene to form ether ylide and then subsequently slowly releasing the carbene, whereupon it eventually reacts with pyridine.

This interpretation (Case 2) cannot explain the ability of dioxane to depress the observed rate constant of pyridine ylide formation for several reasons. This mechanism requires that the rate constant of carbene reaction with pyridine be 10 times smaller than the rate constant of reaction of carbene with dioxane. It seems unreasonable for dioxane to be more nucleophilic than pyridine. In fact, we have measured  $k_{\text{DIOXANE}}$  for **2Cl** in heptane and Freon-113, and it is much less than  $10^6 \text{ M}^{-1} \text{ s}^{-1}$  (Figures 14 and S16, Supporting Information).

In neat dioxane, the formation of pyridine ylide **4Cl** is biphasic. It seems reasonable that nascent dioxane-solvated carbene **2Cl** partitions between reacting with pyridine to form **4Cl** (the fast growth process of Figure 4) and reacting with neat dioxane to form ylide **6Cl**. Although rapid formation of **6Cl** in neat dioxane does not explain why dilute dioxane decreases the rate of formation of pyridine ylide in Freon-113; it can, however, explain the biphasic growth of pyridine ylide in neat dioxane. The slow formation of **4Cl** observed

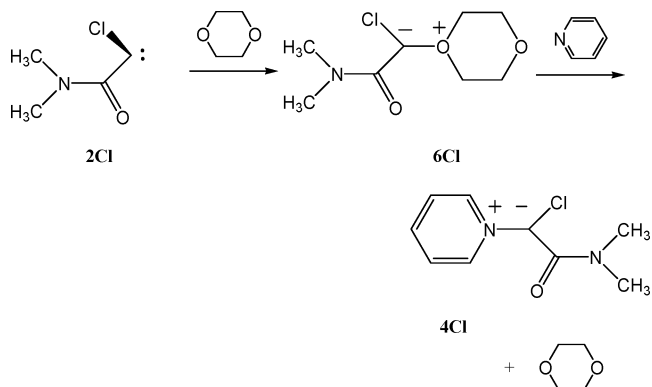
in Figure 4 is consistent with Case 2, slow reversion of ylide to solvated carbene and dioxane.



In this mechanism, the apparent rate constant of ylide **4Cl** formation in dioxane ( $6.8 \times 10^5 \text{ M}^{-1} \text{ s}^{-1}$ , Table 1) will be equal to the value of  $k_{\text{PYR}}K$ , where  $k_{\text{PYR}}$  is the absolute rate constant of the solvated carbene and  $K = [\mathbf{2Cl}][\text{dioxane}]/[\mathbf{6Cl}]$ . Assuming, for the sake of simplicity, that  $k_{\text{PYR}}$  of the carbene in dioxane has the same value as in Freon-113 ( $1.5 \times 10^8 \text{ M}^{-1} \text{ s}^{-1}$ , which we believe is not strictly correct), then we deduce that  $K = 0.0045$  and  $\Delta G = 3.2 \text{ kcal/mol}$  at ambient temperature, in fair agreement with DFT calculations, which predict that  $\Delta H = 8 \text{ kcal/mol}$  for fragmentation of ylide to carbene and ether. In support of this interpretation, we note first that TRIR spectroscopy detects only the presence of ylide in neat THF 200 ns after the laser flash and second that the experimental activation barrier to ylide **4F** formation in THF is close (10.9 kcal/mol) to the enthalpic difference calculated between ylide **4Cl** and carbene **2Cl** and THF (6–8 kcal/mol). Thus, the larger activation energy to pyridine ylide formation observed in THF, relative to Freon-113, while consistent with a Case 1 mechanism seems more consistent with the operation of a Case 2 or 3 in neat THF.

Values of  $k_{\text{DIOXANE}}$  less than  $10^6 \text{ M}^{-1} \text{ s}^{-1}$  (comparable to that determined by TRIR) have no influence on the observed rate constant of formation of pyridine ylide **6Cl**. Of course, one can use KinFitSim to fit the data using any value of  $k_{\text{DIOXANE}}$  (with **2Cl**). Values of  $k_{\text{DIOXANE}}$  ( $k_3$ ) of the order of  $10^6 \text{ M}^{-1} \text{ s}^{-1}$  can be shown to reduce the observed rate of pyridine ylide formation, the key experimental observation, but the *minimum* value of  $k_{\text{DIOXANE}}$  needed to reproduce the experimental effect is much larger than the  $k_{\text{DIOXANE}}$  value determined by TRIR spectroscopy.

**III.3. Ylide Exchange Reaction.** There is a third mechanistic possibility that would allow dioxane to decrease the observed rate constant of formation of pyridine ylide **4Cl**: Case 3. In this mechanism, carbene **2Cl** reacts rapidly and irreversibly with dioxane to form ether ylide **6Cl**. Ether ylide **6Cl** then reacts with pyridine to form pyridine ylide **4Cl** in an ylide exchange reaction, without direct intervention of a carbene.



We cannot rule out the possibility that ylide **6Cl** reacts with pyridine to form ylide **4Cl**, as **6Cl** does react with piperidine

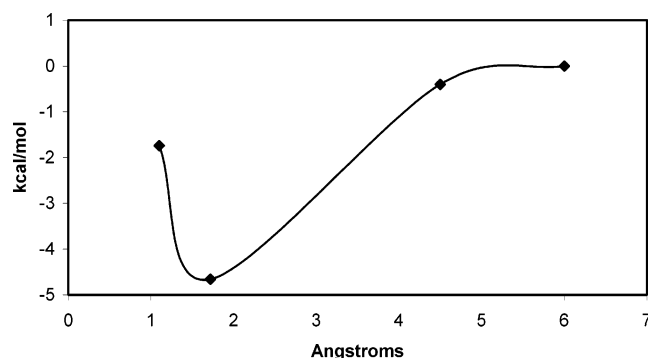


**Figure 18.** PES for dichlorocarbene-dimethyl ether reaction coordinate (MP2/6-31G\*). Infinite separation arbitrarily set to 6 Å.

with a sizable rate constant. This could explain the slow growth of pyridine ylide observed in neat dioxane in LFP experiments. This mechanism, however, cannot explain the decrease in the observed rate of formation of pyridine ylide in the presence of dioxane. To explain the data, the kinetics  $k_{\text{DIOXANE}}$  must still be much larger than  $10^6 \text{ M}^{-1} \text{ s}^{-1}$ .

As mentioned previously, the backside of the ylide is completely shielded by the amide methyl group. Thus, if this mechanism is operative, the nucleophile must approach the ether ylide from out of the plane of the amide, increasing the barrier significantly.

**Potential Energy Surface Predicted by DFT and MP2 Calculations.** We have used calculations at the B3LYP and MP2 levels of theory and the 6-31G\* basis set to examine the reaction of dichlorocarbene with dimethyl ether. These levels of theory find no evidence for the formation of a carbene ether complex corresponding to a stationary point on the potential energy surface (PES). As shown in Figure 18, MP2 theory predicts that the enthalpy will drop continuously between a carbene ether separation of just less than 5 Å until the ylide is formed with a 1.7 Å carbon–oxygen separation. It was necessary to increase the level of theory to obtain a more reasonable carbon–oxygen bond length, as B3LYP/6-311+G\* predicts a carbon–oxygen separation of 2.3 Å for this ylide.

The PES resembles that calculated for the reaction of dichlorocarbene with ethylene.<sup>22</sup> The major difference is that the carbene reaction with ethylene is more than 20 times more exothermic than the reaction of the same carbene with dimethyl ether. This difference explains why dichlorocarbene reacts more rapidly with alkenes than with ethers.<sup>13,15</sup> Both carbene reactions likely traverse free energy barriers dominated by entropic factors.

Figure 19 shows the PES calculated for chlorocarbene amide **2Cl** with dimethyl ether (MP2/6-31G\*). This surface is distinctly different, as it indicates the formation of a weakly bound (3.3 kcal/mol relative to infinite separation) Lewis acid–base complex. The putative complex is a minimum on the PES with a carbon–oxygen separation of 4.1 Å. It should rapidly equilibrate with free carbene and must traverse a barrier of 0.5 kcal/mol to form an ylide. The carbon–oxygen separations for the transition state and ylide are 2.75 and 1.52 Å for the complex and the ylide, respectively. The surface was also calculated at the B3LYP level of theory with the 6-31G\*, 6-31+G\*, and 6-311+G\* basis sets to examine basis set superposition errors.

The results are tabulated in Table S9 in Supporting Information. When compared to the MP2 calculations, B3LYP calculations favor a shallower well ( $\sim 1$  kcal/mol) for the Lewis acid–base complex as well as a larger barrier ( $\sim 2$  kcal/mol) to ylide formation. The two levels of theory also diverge on the overall stability of the ylide. MP2 predicts the ylide to be 17 kcal/mol more stable than infinite separation, compared to the B3LYP prediction of about 4 kcal/mol.

As the chlorocarbene amide approaches dimethyl ether, steric interactions develop as the chlorine atom rotates into the proximal amide methyl group. This explains why the amide is bent  $20^\circ$  from the plane defined by the carbonyl versus that in the free carbene. Thus, the doubly occupied nonbonding orbital enjoys better conjugation with the carbonyl group in the complex relative to the ylide. We speculate that the steric interaction and the deconjugation effect are responsible for the small barrier between the complex and the ylide. The complex must react more slowly with pyridine and TME than free carbene to explain our data. The calculations explain why we see this effect with carbene **2Cl** but not dichlorocarbene, which is not predicted to form a complex.

#### IV. Conclusions

Chloro- and fluorocarbene amides (**2Cl** and **2F**) can be generated by laser flash photolysis of the appropriate tricyclic diene precursor (**1Cl** and **1F**). The carbenes are trapped with pyridine to form ylides **4Cl** and **4F** with  $\lambda_{\text{max}} = 450 \text{ nm}$ . Observation of the ylides allows deduction of carbene lifetimes and their absolute rate constants of reaction with pyridine ( $k_{\text{PYR}}$ ). LFP of **1Cl** and **1F** with IR detection allow direct observation of the carbonyl vibrations of **2Cl** ( $1635 \text{ cm}^{-1}$ ) and **2F** ( $1650 \text{ cm}^{-1}$ ) in Freon-113. In neat THF and dioxane solvents, only the carbene-ether ylides are observed, which have broad vibrations between  $1560$  and  $1610 \text{ cm}^{-1}$ . Small amounts of dioxane decrease the observed rate of formation of pyridine ylides in Freon-113 and, as demonstrated by TRIR spectroscopy, increase the free carbene lifetime. The data indicate that this is due to the specific solvation of the carbene and is not due to ylide formation.

#### V. Experimental Section

**General Methods.**  $^1\text{H}$  NMR spectra were obtained on a Bruker DRX-250 (250 MHz), DRX-400 (400 MHz), or DRX-500 (500 MHz) spectrometers. The GC-MS spectrometer was an HP-6890 Series GC System with an HP-1 methyl siloxane capillary column ( $40.0 \text{ m} \times 100 \mu\text{m} \times 0.20 \mu\text{m}$ ). The gas chromatograph was linked to an HP 5973 mass-selective detector. Tetrahydrofuran and diethyl ether were distilled from sodium and benzophenone under an argon atmosphere. Dioxane was refluxed over sodium for 1 h and then distilled, under an argon atmosphere. Acetonitrile, ethyl acetate, benzene, cyclohexane, and dichloromethane were distilled over  $\text{CaH}_2$  using a 40 cm Vigreux column, under an argon atmosphere. Freon-113 was HPLC grade, purchased from Aldrich, and distilled from  $\text{P}_2\text{O}_5$  under an argon atmosphere.

For LFP studies, 1 mL samples were prepared in quartz cuvettes with an optical density of precursor of 0.1–0.3 at 308 nm. The LFP apparatus utilized was a Lambda Physik LPX 100/200 excimer laser (308 nm, 150 mJ, 17 ns, XeCl excimer). Transient absorption spectra were obtained on an EG&G PARC 1460 optical multichannel analyzer fitted with an EG&G PARC 1304 pulse amplifier, an EG&G PARC 1024 UV detector, and a Jarrell-Ash 1234 grating. The monochromator used was an Oriol 77200. Signals were obtained with a photomultiplier

(22) Houk, K. N.; Rondan, N. G.; Mareda, J. *Tetrahedron* **1985**, *41*, 1555.

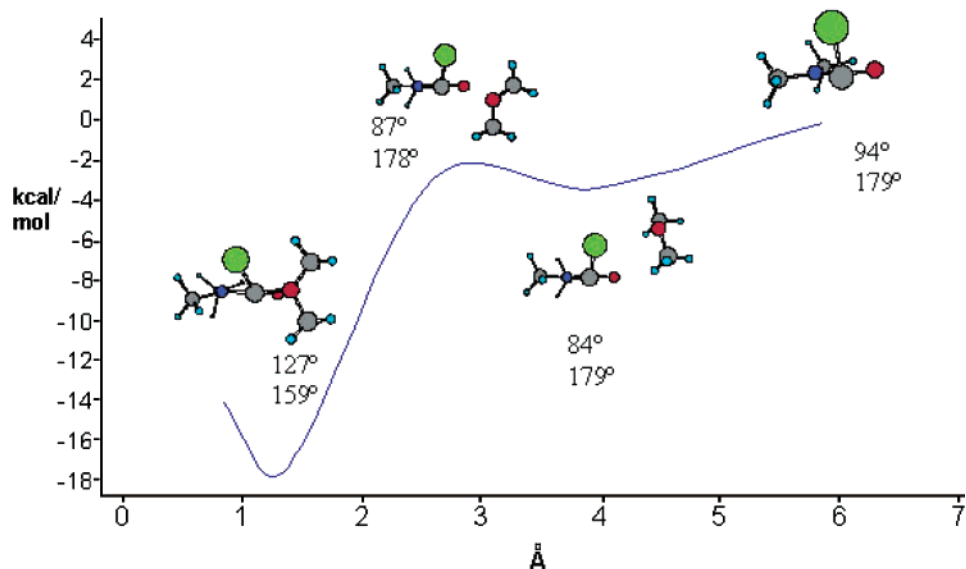


**Figure 19.** PES for chloroamidocarbene-dimethyl ether reaction coordinate (MP2/6-31G\*). Infinite separation arbitrarily set to 6 Å (dihedral angles correspond to Cl–C–C–O (top) and O–C–N–C (bottom) carbene dihedral angles, respectively).

tube detector and digitalized by a Tektonix 5818A A/D transient digitizer. The spectrometer has been described elsewhere in detail.<sup>9</sup>

**10-endo-Fluoro,10'-N,N-dimethylcarboxamidetricyclo[4.3.1.0<sup>1,6</sup>]-deca-2,4-diene (1F).** To a stirred solution of 10-endo-fluoro-10'-exochlorotricyclo[4.3.1.0<sup>1,6</sup>]deca-2,4-diene (750 mg, 0.0033 M) in 30 mL of THF at  $-78\text{ }^{\circ}\text{C}$  was added 1.1 equiv of *n*-BuLi (2.5 M in hexanes). The reaction turned dark blue and was stirred for 1 h. A solution of *N,N*-dimethylchlorocarboxamide (364 mg, 0.0033 M) in 5 mL THF was added to the reaction dropwise via a chilled needle, and the blue color faded gradually. The reaction was stirred for 1 h at  $-78\text{ }^{\circ}\text{C}$ , allowed to warm to ambient temperature, and quenched with 100 mL of water and 100 mL of diethyl ether. The layers were separated, and the aqueous layer was extracted with  $1 \times 100\text{ mL}$  of diethyl ether. The organic layers were combined and dried over  $\text{MgSO}_4$ , filtered, and concentrated on a rotary evaporator to afford an orange tar. This was taken up in a minimum amount of  $\text{CH}_2\text{Cl}_2$  and passed over silica gel with hexanes and then ether/hexanes (1:5). The appropriate fractions were combined to afford crystalline **1F** in 44% yield:  $^{19}\text{F}$  NMR (376 MHz,  $\text{CDCl}_3$ )  $\delta$   $-187.3$ ;  $^1\text{H}$  NMR (500 MHz,  $\text{CDCl}_3$ )  $\delta$  1.2 (m, 2H), 1.91 (m, 2H), 2.46 (m, 2H), 3.03 (d, 3H,  $J = 1.9\text{ Hz}$ ), 3.14 (d, 3H, 1.9 Hz), 5.92 (d, 2H,  $J = 9.7\text{ Hz}$ ), 6.16 (d, 2H,  $J = 9.8\text{ Hz}$ );  $^{13}\text{C}$  NMR (126 MHz,  $\text{CDCl}_3$ )  $\delta$  21.87, 33.47, 35.69, 37.08 (d,  $J_{\text{C-F}} = 11\text{ Hz}$ ), 45.20 (d,  $J_{\text{C-F}} = 42\text{ Hz}$ ), 71.8 (d,  $J_{\text{C-F}} = 913\text{ Hz}$ ), 120.46 (d, 20 Hz), 124.2 (d,  $J_{\text{C-F}} = 6\text{ Hz}$ ), 165.32; HRMS (EI) calcd 221.2707, found 221.1230.

**10-endo-Chloro,10'-N,N-dimethylcarboxamidetricyclo[4.3.1.0<sup>1,6</sup>]-deca-2,4-diene (1C1).** To a stirred solution of 10-endo-dichlorotricyclo[4.3.1.0<sup>1,6</sup>]deca-2,4-diene (680 mg) in THF at  $-78\text{ }^{\circ}\text{C}$  was added 1.1 equiv of *n*-BuLi (2.5 M in hexanes). The reaction turned dark blue and was stirred for 1 h. A solution of *N,N*-dimethylchlorocarboxamide (550 mg) in 5 mL of THF was added to the reaction dropwise, and the blue color faded after 20 min. Following the same workup procedure as for **1F** afforded **1C1** as a white crystalline powder in 38% yield:  $^1\text{H}$  NMR (500 MHz,  $\text{CDCl}_3$ )  $\delta$  1.11 (m, 1H), 1.56 (m, 1H), 2.0 (m, 2H), 2.2 (m, 2H), 2.8 (m, 1H), 3.03 (s, 3H), 3.17 (s, 3H), 5.95 (d, 2H,  $J = 81\text{ Hz}$ ), 6.21 (s, 2H);  $^{13}\text{C}$  NMR (126 MHz,  $\text{CDCl}_3$ )  $\delta$  20.66, 34.19, 34.43, 35.92, 37.38, 38.16, 45.0, 46.73, 121.99, 124.13, 125.51, 168.8; MS (EI) calcd 237.740, found 237.400.

**Adduct (3C1).** Compound **1C1** (26 mg) as a solution in 2,3-dimethyl-2-butene (5 mL) was irradiated with 300 nm light (Ray-O-Net reactor) for 16 h. The mixture was concentrated by rotary evaporation at  $20\text{ }^{\circ}\text{C}$  and eluted over silica gel with hexanes/ether (2:1) to afford **3C1** as a clear oil in 60% yield. Indan peaks were identified by comparison with

authentic material:  $^1\text{H}$  NMR (500 MHz,  $\text{CDCl}_3$ )  $\delta$  1.20 (s, 6H), 1.81 (s, 6H), 2.94 (s, 3H), 3.03 (s, 3H); HRMS ( $\text{M} + \text{Na}$ )<sup>+</sup> calcd 226.09691, found 226.09776.

**Adduct (3F).** Compound **1F** (26 mg) as a solution in 2,3-dimethyl-2-butene (5 mL) was irradiated with 300 nm light (Ray-O-Net reactor) for 15 h. The mixture was concentrated by rotary evaporation at  $20\text{ }^{\circ}\text{C}$  and analyzed by  $^{19}\text{F}$  NMR spectroscopy and mass spectrometry. A yield of 29% was determined by  $^{19}\text{F}$  NMR using 2,3,5,6-tetrafluorotoluene as an internal standard:  $^{19}\text{F}$  NMR (376 MHz,  $\text{CDCl}_3$ )  $\delta$   $-195.53$ ; MS (EI) calcd 185.2244, found 185.100.

**Time-Resolved Infrared (TRIR) Studies.** The TRIR apparatus and technique has been described elsewhere.<sup>23</sup> Briefly, a reservoir of deoxygenated sample solution (10 mL of  $\sim 5\text{ mM}$  **1F** or **1C1**) was continuously circulated in a cell between two barium fluoride salt plates with a 0.5 mm path. The cell was connected to a peristaltic pump by Teflon tubes.

**Density Functional Calculations.** All calculations were carried out with the Gaussian 98 program package.<sup>24</sup> Vibrational frequencies were scaled by a factor of 0.9613.

**Acknowledgment.** Support of this work by the National Science Foundation and the Ohio Supercomputer Center is gratefully acknowledged. E.M.T. gratefully acknowledges GAANN Fellowship Support.

**Supporting Information Available:** Crystallographic details (PDF and CIF). This material is available free of charge via the Internet at <http://pubs.acs.org>.

JA039693K

(23) (a) Yuzawa, T.; Kato, C.; George, M. W.; Hamaguchi, H. *Appl. Spectrosc.* **1994**, *48*, 684. (b) Toscano, J. P. *Adv. Photochem.* **2001**, *26*, 41.

(24) Frisch, M. J.; Trucks, G. W.; Schlegel, H. B.; Scuseria, G. E.; Robb, M. A.; Cheeseman, J. R.; Zakrzewski, V. G.; Montgomery, J. A., Jr.; Stratmann, R. E.; Burant, J. C.; Dapprich, S.; Millam, J. M.; Daniels, A. D.; Kudin, K. N.; Strain, M. C.; Farkas, O.; Tomasi, J.; Barone, V.; Cossi, M.; Cammi, R.; Mennucci, B.; Pomelli, C.; Adamo, C.; Clifford, S.; Ochterski, J.; Petersson, G. A.; Ayala, P. Y.; Cui, Q.; Morokuma, K.; Malick, D. K.; Rabuck, A. D.; Raghavachari, K.; Foresman, J. B.; Cioslowski, J.; Ortiz, J. V.; Stefanov, B. B.; Liu, G.; Liashenko, A.; Piskorz, P.; Komaromi, I.; Gomperts, R.; Martin, R. L.; Fox, D. J.; Keith, T.; Al-Laham, M. A.; Peng, C. Y.; Nanayakkara, A.; Gonzalez, C.; Challacombe, M.; Gill, P. M. W.; Johnson, B. G.; Chen, W.; Wong, M. W.; Andres, J. L.; Head-Gordon, M.; Replogle, E. S.; Pople, J. A. *Gaussian 98*; Gaussian, Inc.: Pittsburgh, PA, 1998.